



Seismic fragility analysis of three-legged jacket supported offshore wind turbine considering ground motion directionality

S. Purkait, U. Nath* & S. Haldar

Indian Institute of Technology Bhubaneswar, Odisha, India

*un13@iitbbs.ac.in

ABSTRACT: Because of growing awareness of the limited availability of fossil fuel resources, the global energy production paradigm has shifted in recent years to the generation of sustainable renewable energy sources, such as wind power. The growing demand for OWTs necessitates their deployment in seismically active regions in deep waters. This highlights the importance of investigating the seismic vulnerability of OWT structures when subjected to seismic loads. The current study examined the seismic fragility of 10 MW wind turbines supported by a three-legged jacketed structure, taking into account the ground motion directionality. A three-dimensional numerical model of three-legged jacket supported OWTs is developed in SAP2000. This study incorporates five near-field and five far-field earthquake motions to analyse the seismic vulnerability of the wind turbine structures. Incremental dynamic analysis (IDA) was used to develop the fragility curves at various angles of ground motion incidence for the considered responses of the structure. Finally, the findings of the study provide useful insight into evaluating the seismic performance of OWTs in order to ensure structural safety and reliability.

Keywords: 3-legged jacket; Ground motion directionality; Incremental dynamic analysis; Seismic fragility

1 INTRODUCTION

Offshore wind is one of the most advanced technologies for producing carbon-neutral energy. The increasing interest in constructing offshore wind farms forced them to install them in earthquake-prone areas due to the lack of appropriate installation areas. Many countries like the United States, China, Japan and some European countries also proposed the installation of offshore wind farms in seismically active regions. This challenge attracts researchers to assess the seismic susceptibility of offshore wind turbines as these tectonically active areas strong earthquakes may affect the design of wind turbines. It has been found that offshore wind turbine with tripod-supported foundations shows better resistance against lateral rotation than monopile-supported offshore wind turbines (Yu et al., 2015).

Various studies have been conducted to study the effect of seismic loading on offshore wind turbine (OWT) structures (Kaynia 2018; Patra and Haldar 2021; James and Haldar 2022). Nevertheless, the effect of near-field pulse-like motions on the responses of the OWT remains unaddressed in these studies. In the near-fault zone, velocity-pulse like records can occur from directivity effects and/or permanent ground displacement because of tectonic movement, referred to as ‘fling-step’ (Bray and

Rodriguez 2004). The significant effects of near-field velocity pulse-like ground motions have been recorded on several occasions, including the Kobe (1995; Japan), Northridge (1994; USA), Wenchuan (2008; China), and Chi-Chi (1999; Taiwan) earthquakes. This highlights the importance of investigating the responses of OWT structures under near-field earthquake motions. Although, very few studies have been conducted to study the effect of pulse-like motions on the dynamic responses of OWT. Ali et al. (2020) performed a cloud-based seismic fragility analysis of monopile supported OWT structures by considering the non-pulse-like and pulse-like ground motions. This study also showed that consideration of the vertical component of the earthquake may induce potential buckling failure of the tower. Sahraeian et al. (2023) investigated the responses of monopile supported OWT under both near-field and far-field ground motions. Their study revealed that the responses of the structure are more critical under near-field earthquake motions due to the presence of high-velocity pulses compared to far-field motions.

Seismic loads make offshore wind turbines more susceptible to damage due to the increased probability of uncertainty associated with this type of load. Therefore, the fragility of the wind turbine structure

must be assessed in relation to seismic loads. Seismic fragility analysis evaluates the risk generated by earthquake loads to assure structural safety. A seismic fragility curve of offshore wind turbines generally indicates the vulnerability of the structure to different seismic events and can be plotted against different intensity measures (IM) of earthquake records. The majority of the studies related to seismic fragility study are available for the buildings, bridges and offshore platforms (Ajamy et al. 2018; Ramamoorthy et al. 2006). However, there is growing interest has been noticed in the field of wind turbines to study the seismic vulnerability associated with this type of structure. Kim et al. (2014) performed seismic fragility analysis of a monopile supported 5 MW offshore wind turbine considering soil-pile interaction, using the fragility function mentioned in Eq. 1.

$$P[D > C|IM] = \Phi \left[\frac{\ln\left(\frac{a}{C_k}\right)}{\xi_k} \right] \quad (1)$$

where $[D > C|IM]$ refers to the probability of exceeding demand for a given intensity measure (IM); C_k and ξ_k are the median and logarithmic standard deviation of a and $\Phi(\cdot)$ denotes the Cumulative Distribution Function (CDF) for normal distribution. Sharmin et al. (2016) investigated the displacement-based fragility analysis at different soil site conditions for jacket supported OWT. De Risi et al. (2018) examined the vulnerability of monopile-supported offshore wind turbines employing unscaled natural earthquakes. The outcome of the study showed that the strong crustal and interface earthquakes cause vulnerable damage to the OWT. It has been observed that in most of the above-mentioned studies, the ground motions applied along the fore-aft and side-side directions of the OWT structure. However, various past studies on the seismic vulnerability of building and bridge structures revealed that the incidence angle of the ground motion events has an important role in the dynamic responses of the structures (Penzien and Watabe, 1974; Athanatopoulou, 2005; Noori et al. 2019). A few studies examined the directionality effect on the seismic responses of the OWT (Moet et al. 2017; Tran et al. 2020). A recent study conducted by Nath and Haldar (2024) demonstrated that the dynamic responses of the jacketed OWTs are sensitive to the directionality effect of the selected ground motions.

A review on literature shows that there is no study to address the vulnerability of 3-legged jacketed OWT is available under near-field pulse like motions. Therefore, this present study attempts to study the seismic vulnerability of the 3-legged jacket-

supported OWT structure under the effect of the near-field pulse-like ground motions. The numerical modelling of the structure is done in SAP2000 considering the ground motion directionality. Moreover, the vulnerability of the structure is also compared under the effect of near-field and far-field ground motions. The study provides valuable insight into evaluating the seismic performance of OWTs supported by the 3-legged jacketed foundation, ensuring their structural safety and reliability.

2 NUMERICAL MODELLING

The three-legged jacket-supported offshore wind turbine has been numerically modelled using beam elements in SAP2000 software. The schematic diagram and 3D finite element model of the three-legged jacket supported OWT has been represented in Fig. 1. The soil profile of Gujarat region, India, is considered in this study according to the feasibility study for offshore wind farm development in Gujarat, India (FOWIND, 2018). A 10 MW reference wind turbine model has been considered for the present study, details of which are obtained from the literature (Bak et al., 2013) presented in Table 1. The dimensions of the three-legged jacket are adopted after modifying the four-legged jacket dimensions from the literature (Brostel 2013). The Rotor Nacelle Assembly (RNA) is modelled at the top of the tower as a lumped mass. The hollow circular steel section with an outer diameter of 2.438m and length of 41.5 m is used for pile sections, as per Brostel (2013).

Due to its simplicity, the API (2011) based p-y curves are widely used in the offshore industry (Risi et al. 2018). The soil springs with nonlinear p-y curves are modelled using multi-linear plastic kinematic link property available in SAP2000. The uniform ground motions are applied at each fixed end of the p-y springs (Risi et al. 2018; Ali et al. 2020).

Table 1. Wind Turbine Data for DTU 10 MW reference wind turbine (Bak et al., 2013).

Properties	Value
Turbine Rated Power	10 MW
Rated Wind Speed	11.4 m/s
Tower bottom diameter	7.665 m
Tower top diameter	5.5 m
Hub height (Above MSL)	119 m
Rotor-Nacelle Assembly (RNA) mass	676.723 tons
Rotor diameter	178.3 m
Moment of inertia about the x-axis of RNA	$1.6 \times 10^8 \text{ kg-m}^2$
Moment of inertia about the y-axis of RNA	$1.27 \times 10^8 \text{ kg-m}^2$
Moment of inertia about the z-axis of RNA	$1.27 \times 10^8 \text{ kg-m}^2$

Table 2. List of near-field ground motions.

Ground motion	Year	Station	PGA (g)		R (km)	T _{pulse} (sec)	M
			Longitudinal	Transverse			
Loma Prieta	1989	Saratoga – Aloha	0.51	0.33	1.35	4.5	6.9
Imperial valley-06	1979	El Centro Array #6	0.45	0.44	1.35	3.77	6.5
Kocaeli	1999	Izmit	0.23	0.17	7.21	5.36	7.5
Irpinia	1980	Sturmo station	0.32	0.23	10.8	3.27	6.9
Chi-Chi	1999	TCU065	0.78	0.57	0.57	5.7	7.6

Table 3. List of far-field ground motions.

Ground motion	Year	Station	PGA (g)		R (km)	M
			Longitudinal	Transverse		
Kobe, Japan	1976	Shin-Osaka	0.23	0.23	19.2	6.9
Manjil, Iran	1990	Abbar	0.51	0.49	12.5	6.9
Northridge-01	1994	Beverly Hills - Mulhol	0.62	0.45	18.4	7.3
San Fernando	1976	LA – Hollywood Stor	0.22	0.19	22.7	6.6
Superstition Hills	1987	El Centro Imp. Co. Cent	0.35	0.26	18.2	6.5

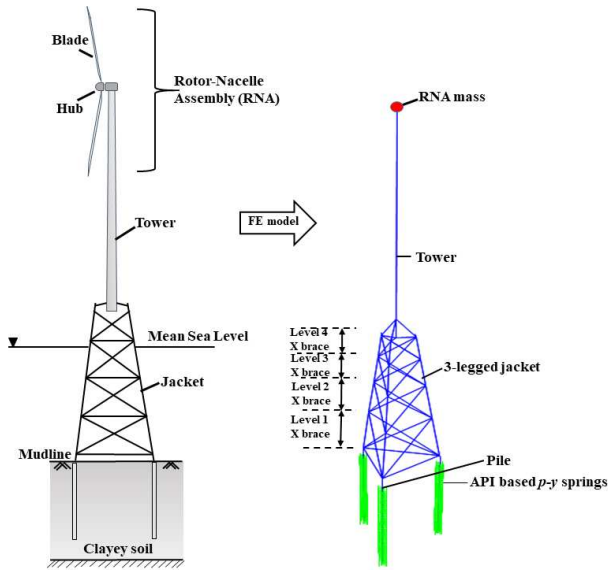


Figure 1. Schematic diagram of 3-legged jacketed OWT and FE model in SAP2000.

3 ANGLE OF INCIDENCE OF GROUND MOTION

The literature on buildings and bridges shows that the angle of incidence of bi-directional motions can greatly affect structure responses. (Reyes and Kalkan 2015). However, limited studies of ground motion directionality are available on the dynamic responses of OWT structure (Mo et al. 2017; Nath and Haldar

2024). Conventionally, the two as-recorded earthquake components are applied along the principal axes of OWT. But, in this study, the recorded ground motions are rotated and applied along the Fore-Aft (FA) and Side-Side (SS) directions simultaneously to account for the directionality effect. A schematic presentation of earthquake components rotated at an angle of ψ is shown in Fig. 2.

$$\begin{Bmatrix} a_x(\psi) \\ a_y(\psi) \end{Bmatrix} = \begin{bmatrix} \cos \psi & \sin \psi \\ -\sin \psi & \cos \psi \end{bmatrix} \begin{Bmatrix} a_x \\ a_y \end{Bmatrix} \quad (2)$$

where a_x and a_y are the recorded horizontal components of the earthquake subjected to the FA and SS direction of OWT; $a_x(\psi)$ and $a_y(\psi)$ are the rotated ground motion components with the structural principal axes. The recorded ground motions are rotated from 0° to 360° with an interval of 30° in this study.

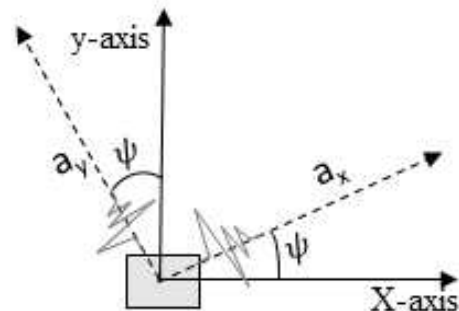


Figure 2. Typical reference axis of OWT structure with rotated ground motion.

4 GROUND MOTION

An ensemble of 10 strong ground motions is selected to assess the vulnerability of 3-legged jacketed OWT. The database comprises five near-field and five far-field records with two horizontal components. The ground motion database is taken from the Federal Emergency Management Agency (FEMA P695, 2009). The same database is also used in Mo et al. (2017). The properties of near-field and far-field motions are provided in Tables 2 and 3, respectively. The pulse period (T_{pulse}) associated with the pulse-like motions is also given in the table. The selected near-field motions are characterised as pulse-like motion based on the wavelet analysis mentioned in Baker (2001). A comparison of the typical velocity-time history of near-field earthquake motion (Imperial Valley, 1979) and far-filed motion (San Fernando, 1976) is shown in Fig. 3.

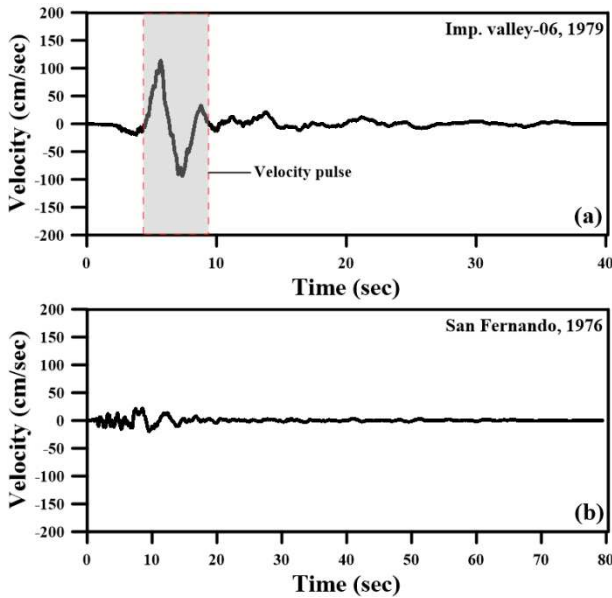


Figure 3. A typical velocity time history of (a) near-field pulse-like (b) far-filed motion.

5 METHODOLOGY

Fragility curves are used to represent the vulnerability of structures as probability functions of earthquake ground motion intensity. Seismic fragility is defined as the probability that the structural demand (D) surpasses the structural capacity (C) for a given ground motion intensity measure (Kennedy et al., 1980). Assuming both the structural capacity and demand follow the lognormal distribution, seismic fragility can be modelled as a lognormal probability distribution function as described in Eq. 1 (Baker 2015). Incremental dynamic analysis

proposed by Vamvatsikos and Cornell (2002) is adopted to develop the fragility curves of the structure. This present study considers peak ground acceleration (PGA) as IM value mentioned in existing literature (Mo et al. 2017). Two limit states (LSs) are considered in this study, corresponding to the tower-top displacement (u_t) and tower-top rotation (θ_t). The permissible limits of the two considered limit states are provided in Table 4 (Mo et al. 2017; Asareh et al. 2016).

Table 4. Limit states considered in this study

Limit States	Permissible value
Tower-top displacement (LS ₁)	1.25% of the tower's height
Tower-top rotation (LS ₂)	2.5°

6 RESULT AND DISCUSSIONS

6.1 Fragility considering ground motion directionality

Fig. 4 presents the fragility curves of a 10 MW 3-legged jacketed OWT for near-field and far-field ground motions accounting for the ground motion incidence angles. The fragility curves are generated for 0° to 360° angle of incidence. However, the lowest and the highest fragility curves corresponding to the orientation are shown in the present paper for the brevity of the paper.

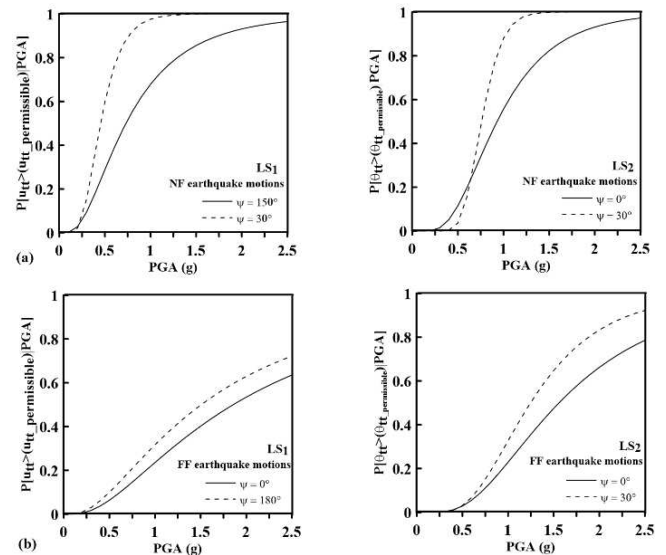


Figure 4. Fragility curves of 3-legged jacketed foundation for (a) near-field and (b) far-field ground motions considering ground motion directionality for LS₁ and LS₂

It can be depicted from Fig. 4 that the vulnerability is more in other directions compared to

0° angle of incidence. In the case of LS1, the structure is more vulnerable to 30° angle of orientation. However, the lower bound of vulnerability is observed for a 150° angle of incidence. For example, for a moderate earthquake level of 0.5g, the probability of exceedance (PoE) for tower-top displacement is 25% and 45% for 150° and 30° angle of incidence. The fragility curve for tower-top rotation is more for severe earthquake levels of 0.8g at 30° angle of incidence for near-field seismic motions. At a PGA level of 1g, the PoE is 73% for the angle of orientation of 30°, whereas the PoE is 45% for 0° angle of incidence. This shows an increment of almost 62% in the fragility curve when compared to the 0° angle of orientation. A similar trend is also noticed in the case of far-field motion (cf. Fig. 4(b)). However, the directionality effect is marginal in the case of far-field motions for LS₂ when compared to the 0° orientation of earthquake excitation. This highlights the importance of considering the ground motion directionality into account to ensure the safety and stability of the structure.

6.2 Comparison of fragility curves for near-field and far-field motions

The fragility curves generated for near-field and far-field motions are compared in this present section and also shown in Fig. 5.

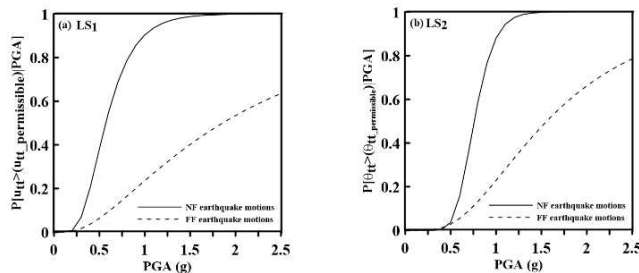


Figure 5. Comparison of the fragility of OWT for (a) LS1 and (b) LS₂ under near-field and far-field motions.

It is evident that LS₁ is more vulnerable under near-field motions compared to the far-field motions (cf. Fig. 5 (a)). To further address this point, PoE for three PGA levels such as 0.2g (low), 0.5g (moderate), and 0.8g (severe), are considered for comparing the responses under near-field and far-field earthquake excitations. In the case of low earthquake levels, a negligible difference is observed for near-field and far-field motions. The PoE is almost 12% for far-field motions. However, the PoE reaches to almost 50% in the case of near-field earthquake motions for 0.5g level of earthquake shaking. The difference is more prominent in cases of severe ground motion

excitation. The PoE is almost 90% under near-field earthquake motions, whereas the probability is only about 20% for far-field motions. The structure also shows more vulnerability under near-field motions for LS₂. The probable reason behind the higher responses of the structure under near-field motions could be the higher level of energy associated with the velocity pulses with larger periods. These pulses can exert a higher lateral force on the structure, leading to higher responses for a given PGA level. A similar trend is also noticed in Sahraeian et al. (2023). However, a higher number of ground motion records is required to enhance the accuracy of the fragility curve.

7 CONCLUSIONS

This study develops seismic fragility curves for 10 MW OWT supported by the 3-legged jacketed foundation under near-field and far-field earthquake motions. Moreover, the fragility curves are also generated for the structure considering ground motion directionality. The numerical modelling of the structure is done in SAP2000. Incremental dynamic analysis (IDA) is carried out to develop the fragility curves for the structure. Some important observations can be noticed from the present study are given below:

- (1) It is observed that the 3-legged jacket structure is highly sensitive to the effect of ground motion directionality. The limit state, corresponding to tower-top rotation, shows an increment of almost 62% at an angle of orientation of 30° when compared to 0° angle of incidence for near-field earthquake motions. The tower-top displacement is also more vulnerable in case of 30° angle of orientation. This highlights the importance of accounting for ground motion directionality to ensure structural safety.
- (2) The responses are highly vulnerable in the case of near-field motions compared to far-field motions. Low-intensity near-field and far-field earthquake motions show less variability in responses. However, the variability increases for moderate to high intensity earthquake motions in the case of near-field motions when compared to far-field motions.

AUTHOR CONTRIBUTION STATEMENT

Sagnik purkait: Methodology, Formal analysis, Writing - original draft. Upasana Nath: Visualization, Conceptualization, Writing - original draft. Sumanta Haldar: Writing – review and editing, Supervision, Conceptualization.

REFERENCES

- Asareh, M.A., Schonberg, W., Volz, J. (2016). Fragility analysis of a 5-MW NREL wind turbine considering aero-elastic and seismic interaction using finite element method. *Finite Elem. Anal. Des.*, 120:57–67.
- Athanatopoulou, A.M. (2005). Critical orientation of three correlated seismic components. *Engineering Structures* 27:301–312.
- Ali, A., R. De Risi, Sextos, A., Goda, K., Chang, Z. (2020). Seismic vulnerability of offshore wind turbines to pulse and nonpulse records. *Earthquake Eng. Struct. Dyn.* 49 (1): 24–50.
- Ajamy, A., Asgarian, B., Ventura, C.E., Zolfaghari, M.R. (2018) Seismic fragility analysis of jacket type offshore platforms considering soil-pile-structure interaction. *Eng. Struct* 174:198–211.
- Bray, J.D., Rodriguez, M.A. (2004) Characterization of forward-directivity ground motions in the near-fault region. *Soil Dyn Earthq Eng* 24(11):815–28.
- Bak C, Zahle F, Bitsche R, Kim T, Yde A, Henriksen LC, et al. (2013) Description of the DTU 10 MW reference wind turbine. DTU Wind Energy Report-I-0092;5.
- Borstel, V., Schumann, B. (2013). INNWIND.EU Design Report-Reference Jacket, D4.3.1.
- Baker J. (2015). Efficient analytical fragility function fitting using dynamic structural analysis. *Earthquake Spectra*, 31:579–599.
- Baker, J.W. (2007). Quantitative classification of near-fault ground motions using wavelet analysis. *Bull Seismol Soc Am*, 97:1486–501.
- De Risi, R., Bhattacharya, S., Goda, K. (2018). Seismic performance assessment of monopile-supported offshore wind turbines using unscaled natural earthquake records. *Soil Dynam. Earthq. Eng.* 109, 154–172.
- FEMA P695 (2009). Quantification of building seismic performance factors. Federal Emergency Management Agency.
- FOWIND (2018). Concept wind farm design, Feasibility study for offshore wind farm development in Gujarat.
- James, M., Haldar, S. (2022). Seismic Vulnerability of Jacket Supported large Offshore Wind Turbine Considering Multi-Directional Ground Motions. *Structures*. 43:407–423.
- Kaynia, A.M. (2018). Seismic considerations in the design of offshore wind turbines. *Soil Dyn Earthq Eng.*, 124:399–407.
- Kennedy, R.P., Cornell, C.A., Campbell, R.D., Kaplan, S., Perla, H.F. (1980). Probabilistic seismic safety study of an existing nuclear power plant. *Nucl. Eng. Des.* 59 (2), 315–338.
- Kim, D.H, Lee, S.G, Lee, I.K. (2014). Seismic fragility analysis of 5 MW offshore wind turbine. *Renew Energy* 65:250–6.
- Mo R, Kang H, Li M, Zhao X. (2017). Seismic fragility analysis of monopile offshore wind turbines under different operational conditions. *Energies*, 10:1037.
- Noori, H.R., Memarpour, M.M., Yakhchalian, M., Soltanieh, S. (2019). Effects of ground motion directionality on seismic behaviour of skewed bridges considering SSI. *Soil Dynam. Earthq. Eng.* 127, 105820.
- Nath, U., Haldar, S. (2024). Effectiveness of combination rule at predicting the elastic seismic demand of jacket-supported offshore wind turbine subjected to bi-directional motions. *Structures*. 64:106455.
- Penzien, J., Watabe, M. (1974). Characteristics of 3-dimensional earthquake ground motions. *Earthq. Eng. Struct. Dynam.* 3(4):365–373.
- Patra, S. K., Haldar, S. (2021). Seismic performance of multi-megawatt offshore wind turbines in liquefiable soil under horizontal and vertical motions. *Int. J. Geomech.* 39:1411–1432.
- Ramamoorthy, S.K, Gardoni, P, Bracci, J.M. (2006). Probabilistic demand models and fragility curves for reinforced concrete frames. *J. Struct. Eng.* 132(10):1563–1572.
- Reyes, J.C., Kalkan, E. (2015). Significance of rotating ground motions on the behaviour of symmetric- and asymmetric-plan structures: Part I. Single-story structures. *Earthq Spectra*, 31:1591–612.
- Sahraeian, S.M., Masoumi, M.A., Najafgholipour, M.A., Shafiee, A., Pandey, B. (2023). Seismic response of monopile foundation of offshore wind turbines under near-field and far-field ground motions. *Soil Dyn Earthq Eng.*, 174:108166.
- Vamvatsikos D. and Cornell C.A. (2002). Incremental Dynamic Analysis. *Earthquake Engineering and Structural Dynamics*, Vol. 31, Issue 3, pp. 491-514.

INTERNATIONAL SOCIETY FOR SOIL MECHANICS AND GEOTECHNICAL ENGINEERING



This paper was downloaded from the Online Library of the International Society for Soil Mechanics and Geotechnical Engineering (ISSMGE). The library is available here:

<https://www.issmge.org/publications/online-library>

This is an open-access database that archives thousands of papers published under the Auspices of the ISSMGE and maintained by the Innovation and Development Committee of ISSMGE.

The paper was published in the proceedings of the 5th International Symposium on Frontiers in Offshore Geotechnics (ISFOG2025) and was edited by Christelle Abadie, Zheng Li, Matthieu Blanc and Luc Thorel. The conference was held from June 9th to June 13th 2025 in Nantes, France.